Published in IET Communications
Received on 1st May 2012
Revised on 1st October 2012
Accepted on 10th November 2012
doi: 10.1049/iet-com.2012.0232

ISSN 1751-8628

Expected complexity analysis of increasing radii algorithm by considering multiple radius schedules

Junil Ahn[1,2], *Heung-No Lee*[1], *Kiseon Kim*[1]

[1]*School of Information and Mechatronics (SIM), Department of Nanobio Materials and Electronics, WCU, Gwangju Institute of Science and Technology (GIST), 1 Oryong-dong, Buk-gu, Gwangju 500-712, Republic of Korea*
[2]*Agency for Defense Development, 111 Sunam-dong, Yuseong-gu, Daejeon 305-152, Republic of Korea*
E-mail: junilahn98@gmail.com

Abstract: In this study, the authors investigate the expected complexity of increasing radii algorithm (IRA) in an independent and identified distributed Rayleigh fading multiple-input–multiple-output channel with additive Gaussian noise and then present its upper bound result. IRA employs several radii to yield significant complexity reduction over sphere decoding, whereas performing a near-maximum-likelihood detection. In contrast to the previous expected complexity presented by Gowaikar and Hassibi (2007), where the radius schedule was hypothetically fixed for analytic convenience, a new analytical result is obtained by considering the usage of multiple radius schedules. The authors analysis reflects the effect of the random variation in the radius schedule and thus provides a more reliable complexity estimation. The numerical results support their arguments, and the analytical results show good agreement with the simulation results.

1 Introduction

In general, the maximum-likelihood (ML) detection of symbols over the underlying lattice structure is interpreted as an integer least-squares (ILS) problem [1, 2]. The ILS problem frequently arises in communication applications such as ML detection for multiple-input–multiple-output (MIMO) systems [3–5], ML multiuser detection for code-division multiple access (CDMA) systems [6], and ML sequence estimation [7]. For arbitrary channels, the exhaustively solving of the ILS problem is known to be NP-hard [8, 9].

During the last decade, sphere decoding (SD) has attracted significant interest as a detection scheme for solving the ILS problem. This is because SD provides the optimal ML performance with moderate average complexity, especially for MIMO channels [3–5]. In essence, SD limits the search space to within a single radius and then performs a depth-first tree search over a tree with as many depths as the system dimension (i.e. the number of transmit antennas in MIMO context) [3]. However, as the system dimension or the constellation size increases, SD tends to be impractical because the SD complexity grows exponentially in both the worst and average senses. To alleviate this problem, increasing radii algorithm (IRA) [10] and its extensions [11, 12] have been proposed. Instead of a single radius, IRA adopts several radii during a depth-first tree search. Subsequently, it has lower complexity than SD as well as maintains a near-ML performance.

The complexity of depth-first tree search-based algorithms such as SD and IRA is a random variable that depends on distributions of the channel, noise and transmitted symbol. Thus, several works in the literature have focused on quantifying the expected complexity of the algorithm in order to characterise complexity behaviour; for example, the authors in [1, 13] analysed the expected complexity of SD and a SD variant based on the l^{∞}-norm, respectively. Especially, in [10], the expected complexity of IRA given for one fixed radius schedule (which indicates a set of radii) has been defined, and its upper bound has been analysed in order to support the complexity reduction of IRA over SD. However, in fact, this upper bound is obtained only for a single fixed radius schedule.

In practice, IRA utilises multiple radius schedules to guarantee a non-vanishing probability of detecting a symbol. It makes gear shifts from one radius schedule to the next whenever it encounters a random search failure. Accordingly, the IRA complexity changes depending on the variation in the radius schedule. Although fixing the radius schedule simplifies the analysis procedure, the complexity analysis for one fixed radius schedule does not completely reflect the practical complexity of IRA. In order to address this issue, we present a new IRA complexity expression that considers the effect of the realistic variation in the radius schedule. Subsequently, instead of using the exact analysis, which seems to be intractable in this case, we investigate the upper bound on the expected IRA complexity using the proposed complexity expression and our analytic findings. Numerical results support the idea that the new complexity analysis allows us to predict the IRA complexity without ambiguity with respect to the radius schedule. Therefore in practice, the obtained analytical results can be used to reliably estimate complexity under any setting of radius schedule.

The remainder of this paper is organised as follows: In Section 2, the system model and IRA are briefly described. Section 3 presents the new expected complexity expression for IRA and its upper bound analysis. In Section 4, numerical results that support our arguments are discussed. Finally, we conclude this paper in Section 5.

2 System model and increasing radii algorithm

The ILS problem, which amounts to the ML detection in a MIMO system with M transmit antennas and N receive antennas ($N \geq M$), is formulated as

$$\hat{\boldsymbol{x}}_{\mathrm{ML}} = \arg\min_{\boldsymbol{x}\in\mathcal{S}^M} \left\| \boldsymbol{Q}^*\boldsymbol{y} - \boldsymbol{R}\boldsymbol{x} \right\|^2 \tag{1}$$

$$\text{subject to } \boldsymbol{y} = \boldsymbol{H}\bar{\boldsymbol{x}} + \boldsymbol{z} \tag{2}$$

where $\boldsymbol{y} \in \mathcal{C}^N$ is the received vector, $\mathcal{C}^N$ is the set of all complex $N \times 1$ vectors, $\boldsymbol{z} \in \mathcal{C}^N$ denotes an independent and identically distributed (i.i.d.) zero-mean additive complex Gaussian noise vector, that is $z_i \sim \mathcal{CN}(0, \sigma_z^2)$, $\boldsymbol{H} \in \mathcal{C}^{N\times M}$ is the i.i.d. Rayleigh fading MIMO channel matrix of column full rank, $\mathcal{C}^{N\times M}$ is the set of all complex $N \times M$ matrices, the entries of $\boldsymbol{H} \sim$ i.i.d. $\mathcal{CN}(0, \sigma_h^2)$, $\boldsymbol{H} = \boldsymbol{Q}\boldsymbol{R}$ by the QR-decomposition of $\boldsymbol{H}$, $\boldsymbol{Q}$ is an $N \times M$ unitary matrix, and $\boldsymbol{R}$ is an $M \times M$ upper triangular matrix with non-negative diagonal entries. The transmitted vector $\bar{\boldsymbol{x}} \in \mathcal{S}^M$ is independently and equally likely drawn from an M-dimensional L^2-QAM constellation $\mathcal{S}^M$ with an even number L such that

$$\mathcal{S}^M = \left\{ s_1 + js_2 | s_1, s_2 \in \left\{ -\frac{L-1}{2}, -\frac{L-3}{2}, \ldots, \frac{L-3}{2}, \frac{L-1}{2} \right\} \right\}^M$$

and $\boldsymbol{x} \in \mathcal{S}^M$ is the candidate vector. The received signal-to-noise ratio (SNR) γ in (2) is given by

$$\gamma = \frac{\mathbb{E}\left(\|\boldsymbol{H}\bar{\boldsymbol{x}}\|^2\right)}{\mathbb{E}\left(||\boldsymbol{z}||^2\right)} = \frac{M(L^2-1)\sigma_h^2}{6\sigma_z^2}$$

where $\mathbb{E}(\cdot)$ is the expectation operation.

As the upper triangularity of $\boldsymbol{R}$ in (1), one can construct a tree of depth M, where branches at depth k ($k = 1, 2, \ldots, M$) correspond to the possible values of x_{M-k+1}, paths from depth 1 to k refer to points $\boldsymbol{x}^{(k)}$ in the lattice $\mathcal{S}^k$ of dimension k, and $\boldsymbol{x}^{(k)}$ stands for the subvector having the last k entries of $\boldsymbol{x}$, that is, $\boldsymbol{x}^{(k)} = [x_{M-k+1}, x_{M-k+2}, \ldots, x_M]^{\mathrm{T}}$. By denoting $\boldsymbol{w} = \boldsymbol{Q}^*\boldsymbol{y} - \boldsymbol{R}\boldsymbol{x}$, a path metric from depth 1 to k in the tree is given by

$$P_k\left(\boldsymbol{x}^{(k)}\right) = \sum_{i=1}^{k} B_i\left(\boldsymbol{x}^{(i)}\right) \tag{3}$$

where $B_i(\boldsymbol{x}^{(i)}) = |w_{M-i+1}|^2$ is a branch metric at depth i.

IRA performs a depth-first tree search using a sequence of increasing radii such that $r_{1,\rho} < r_{2,\rho} < \cdots < r_{M,\rho}$, whereas SD employs only one large radius d over the entire depths in the tree (refer to Fig. 1). Accordingly, IRA explores only the $\boldsymbol{x}^{(k)}$ that satisfy the following condition at each depth k

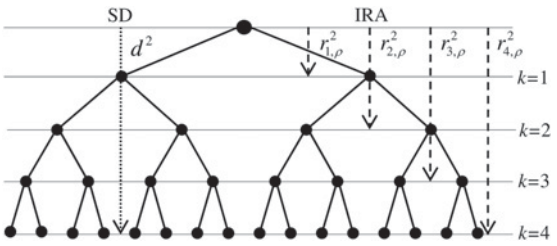

Fig. 1 *Employment strategy of a radius or radii for a depth-first tree search in SD and IRA*

$$P_k\left(\boldsymbol{x}^{(k)}\right) \leq r_{k,\rho}^2, \quad \text{for } k = 1, 2, \ldots, M \tag{4}$$

where $r_{k,\rho}$ is the predefined radius of the radius schedule index ρ, $\rho = 1, 2, \ldots, N_s$, and N_s denotes the total number of radius schedules. The radius schedule with index ρ indicates a set of M radii, that is $\{r_{k,\rho} | k = 1, 2, \ldots, M\}$. In practical applications, IRA employs multiple radius schedules to ensure symbol detection with high probability. Essentially, $r_{k,\rho}$ s are determined such that

$$r_{k,\rho} < r_{k+1,\rho} \text{ for each } \rho \text{ and } r_{k,\rho} < r_{k,\rho+1} \text{ for each } k \tag{5}$$

We refer to $\mathcal{D}_{k,\rho}$ as the search space including all the points $\boldsymbol{x}^{(k)}$ that comply with condition (4) from depth 1 to k in the radius schedule with index ρ. According to the radii selection rule in (5), it holds that $\mathcal{D}_{k,\rho} \subseteq \mathcal{D}_{k+1,\rho}$ for each ρ and that $\mathcal{D}_{k,\rho} \subseteq \mathcal{D}_{k,\rho+1}$ for each k.

IRA finds all the candidates $\boldsymbol{x} \in \mathcal{D}_{M,\rho}$ by consecutively examining (4) from $k = 1$ to M; then, among those survived, the $\boldsymbol{x}$ having the smallest full path metric $P_M(\boldsymbol{x}^{(M)})$ is declared as the final output. When IRA succeeds in search with a radius schedule having index ρ, the corresponding search space is not empty, that is $\mathcal{D}_{M,\rho} \neq \emptyset$. Otherwise, it is empty, that is $\mathcal{D}_{M,\rho} = \emptyset$. When IRA fails in finding a feasible solution with the radius schedule index ρ, it restarts using the next radius schedule with index $\rho + 1$, which includes larger radii than the previous radius schedule. This procedure continues until the final solution is found.

In addition, the original IRA employs $r_{k,\rho}^2 = (\delta(\varepsilon_\rho)\log M + k)\sigma_z^2$ for each k and ρ, where ε_ρ is the user-selected probability and $\delta(\varepsilon_\rho)$ is the scaling factor [10]. Note that ε_ρ should be assigned in a decreasing fashion, that is $\varepsilon_\rho > \varepsilon_{\rho+1}$, in order for the radii to follow the condition $r_{k,\rho} < r_{k,\rho+1}$. In order to maintain coherence with the original IRA, we also perform the following analysis for the ε_ρ and $r_{k,\rho}$ that satisfy the aforementioned conditions.

3 Expected complexity analysis

In this section, we present a new complexity expression for IRA that takes account of multiple radius schedules and their random variations. Thereafter, we establish the upper bound on the expected IRA complexity using our theoretical findings.

doi: 10.1049/iet-com.2012.0232

3.1 Previous expected complexity analysis

In [10], the expected complexity of IRA was defined in ([10], 17) and is rewritten as

$$\sum_{k=1}^{M} E_p(k) f(k) \tag{6}$$

where $E_p(k)$ denotes the expected number of points $\boldsymbol{x}^{(k)}$ in $\mathcal{D}_{k,\rho}$ corresponding to depth k, and $f(k)$ is the number of floating point operations (FLOPs) needed to search for each point at depth k ($f(k) = 8k + 32$ for IRA). Note that, instead of $\mathcal{D}_k$ as used in ([10], 17), we use the notation $\mathcal{D}_{k,\rho}$ to clarify the different size of the search space in each radius schedule with index ρ. The authors of [10] presented the upper bound on (6), which is expressed as

$$\sum_{k=1}^{M} \sum_{x^{(k)}} \Pr\left(P_k\left(\boldsymbol{x}^{(k)}\right) \le r_{k,\rho}^2\right) f(k) \tag{7}$$

where $\sum_{x^{(k)}}$ denotes the sum over all possible $x^{(k)}$, indicating the realisation of $\boldsymbol{x}^{(k)}$.

In (6) and (7), the complexity given for a certain ρ is considered. This implies that in [10], the radius schedule was fixed as one certain set, even though factually, the radius schedule randomly changes during the search procedure. This was done for analytical convenience. Thus, when evaluating the upper bound in (7), ρ should be determined as a specific value between 1 and N_s, even though a strategy to select a proper value of ρ for computing (7) was not clearly specified in [10].

In fact, the value of ρ that provided the analysis result closest to the simulated one was selected after computer simulations in order to evaluate the upper bound in [10]. Subsequently, the numerical trend of the expected complexity was presented as a function of SNR. Fig. 2 shows the analysis results of (7) with several values of ρ for system configurations identical to those for Fig. 7*a* in [10]. The analysis result for $\rho = 1$ in Fig. 2 indicates the upper bound, just as shown in Fig. 7*a* in [10]. In Fig. 2, even though the analysis result for $\rho = 1$ appears tight as the upper bound with respect to the simulation result by chance, this complexity evaluation does not support a reliable complexity estimation without empirical experiments. Therefore this issue needs to be resolved in order to serve the original purpose of the complexity analysis.

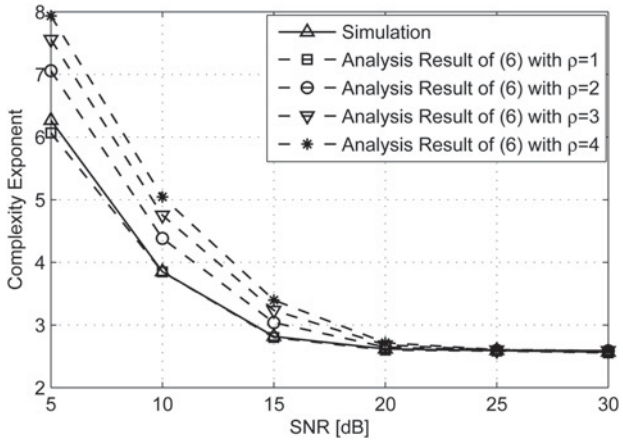

Fig. 2 *Expected complexity in a system with $M = N = 20$ and $L = 2$*

3.2 Expected complexity considering multiple radius schedules

We restate that IRA employs multiple radius schedules and shifts the radius schedule to the next one whenever a random search failure occurs. As the size of the search space $\mathcal{D}_{k,\rho}$ is different for each radius schedule, the IRA complexity changes according to the radius schedule variation. Motivated by this, we aim to demonstrate (i) the use of multiple radius schedules and (ii) the realistic variation in the radius schedule, in the complexity analysis procedure.

Instead of the previously used complexity definition (6), we present a new expression of the expected IRA complexity C as follows

$$C \triangleq \sum_{\rho=1}^{N_s} w(\rho) \sum_{k=1}^{M} \mathbb{E}(N(k, \rho)) f(k) \tag{8}$$

where the expectation is with respect to the channel $\boldsymbol{H}$, noise $\boldsymbol{z}$ as well as transmitted vector $\bar{\boldsymbol{x}}$; $N(k, \rho)$ is the number of points $\boldsymbol{x}^{(k)}$ included in $\mathcal{D}_{k,\rho}$; and $w(\rho)$ is the computational weight in the radius schedule with index ρ. The computational weight is discussed in detail in Section 3.3. Note that in (8), the radius schedule is not fixed artificially, and thus, the new complexity expression (8) can reflect the computational impact from the usage of multiple radius schedules.

Let us consider the expectation term $\mathbb{E}(N(k, \rho))$ in (8). First, we introduce the indicator function, $\mathbf{1}_{\{A\}}$, to count all the points contained in the search space $\mathcal{D}_{k,\rho}$, where $\mathbf{1}_{\{A\}}$ equals 1 if the event A occurs and is 0 otherwise. By using this indicator function and taking a summation over all the possible points, $N(k, \rho)$ is given by $N(k, \rho) = \sum_{\boldsymbol{x}^{(k)}} \mathbf{1}_{\{\boldsymbol{x}^{(k)} \in \mathcal{D}_{k,\rho}\}}$; thus, we obtain the following expression:

$$\begin{aligned} \mathbb{E}(N(k, \rho)) &= \sum_{\boldsymbol{x}^{(k)}} \mathbb{E}\left(\mathbf{1}_{\{\boldsymbol{x}^{(k)} \in \mathcal{D}_{k,\rho}\}}\right) \\ &= \sum_{\boldsymbol{x}^{(k)}} \Pr\left(\boldsymbol{x}^{(k)} \in \mathcal{D}_{k,\rho}\right) \end{aligned} \tag{9}$$

where the last equality comes from $\mathbb{E}(\mathbf{1}_{\{A\}}) = \Pr(A)$. From the definition of $\mathcal{D}_{k,\rho}$, $\Pr(\boldsymbol{x}^{(k)} \in \mathcal{D}_{k,\rho})$ in (9) is equivalent to $\Pr(P_1(x^{(1)}) \le r_{1,\rho}^2, P_2(x^{(2)}) \le r_{2,\rho}^2, \ldots, P_k(x^{(k)}) \le r_{k,\rho}^2)$ whose computation includes a very involved integral, making the exact evaluation of $\Pr(\boldsymbol{x}^{(k)} \in \mathcal{D}_{k,\rho})$ seems extremely intractable. Therefore instead of the exact analysis, we aim to pursue an upper bound on the expected IRA complexity C (8). Subsequently, by using the upper bound $\Pr(\boldsymbol{x}^{(k)} \in \mathcal{D}_{k,\rho}) \le \Pr(P_k(\boldsymbol{x}^{(k)}) \le r_{k,\rho}^2)$ together with (9), we obtain the upper bound on $\mathbb{E}(N(k, \rho))$, which is as follows

$$\mathbb{E}\left(N(k, \rho)\right) \le \sum_{\boldsymbol{x}^{(k)}} \Pr\left(P_k\left(\boldsymbol{x}^{(k)}\right) \le r_{k,\rho}^2\right) \tag{10}$$

Then, by incorporating (10) into (8), the expected complexity C (8) is found to be upper bounded by

$$C \le \sum_{\rho=1}^{N_s} w(\rho) \sum_{k=1}^{M} \sum_{\boldsymbol{x}^{(k)}} \Pr\left(P_k\left(\boldsymbol{x}^{(k)}\right) \le r_{k,\rho}^2\right) f(k) \tag{11}$$

In the above equation, we directly established the upper bound on the new complexity expression (8), instead of the

complexity given for one fixed ρ (6). Thus, although the new upper bound is given as a weighted sum of (7), it is intrinsically different from the previous upper bound. The numerical results presented in Section 4 also show this difference between the new and previous upper bounds.

3.3 Computational weight in radius schedule

Now, we investigate the computational weight in the radius schedule having index ρ, that is $w(\rho)$ in (11). The weight $w(\rho)$ needs to be designed to reflect the radius schedule variation caused by search failure events. To achieve this and also trace the upper complexity bound, we determine the weight $w(\rho)$ as the upper bound on the search success probability in the radius schedule having index ρ as follows (see Appendix 1)

$$w(\rho) = P_{\mathrm{UB},\rho-1} - P_{\mathrm{LB},\rho} \tag{12}$$

where

$$P_{\mathrm{LB},\rho} = \Pr\left(P_1\left(\boldsymbol{x}^{(1)}\right) > r_{1,\rho}^2\right) \tag{13}$$

and

$$\begin{aligned} P_{\mathrm{UB},\rho-1} = {} & \Pr\left(P_1\left(\boldsymbol{x}^{(1)}\right) > r_{1,\rho-1}^2\right) \\ & + \sum_{k=2}^{M} \Pr\left(P_k\left(\boldsymbol{x}^{(k)}\right) > r_{k,\rho-1}^2\right) \\ & \Pr\left(P_{k-1}\left(\boldsymbol{x}^{(k-1)}\right) \le r_{k-1,\rho-1}^2\right) \end{aligned} \tag{14}$$

with $P_{\mathrm{UB},0} = 1$ by definition. $P_{\mathrm{LB},\rho}$ and $P_{\mathrm{UB},\rho-1}$ can be computed for 4-QAM and 16-QAM constellations, respectively, using (13) and (14) together with (15) and (16) in the following theorem (Theorem 1); note that $\Pr(P_k(\boldsymbol{x}^{(k)}) > r_{k,\rho}^2) = 1 - \Pr(P_k(\boldsymbol{x}^{(k)}) \le r_{k,\rho}^2)$.

Theorem 1: $\Pr(P_k(\boldsymbol{x}^{(k)}) \le r_{k,\rho}^2)$ for the 4-QAM constellation is given by

$$\Pr\left(P_k\left(\boldsymbol{x}^{(k)}\right) \le r_{k,\rho}^2\right) = \sum_{q=0}^{2k} \frac{\binom{2k}{q}}{4^k} \gamma\left(\frac{r_{k,\rho}^2}{\sigma_z^2 + \sigma_h^2 q}, k\right) \tag{15}$$

and for the 16-QAM constellation, it is given by

$$\begin{aligned} \Pr\left(P_k\left(\boldsymbol{x}^{(k)}\right) \le r_{k,\rho}^2\right) = {} & \sum_{q=0}^{18k} \sum_{l=0}^{2k} \frac{\binom{2k}{l}}{4^k} \\ & \frac{\Phi_{2k,l}(q)}{\sum_j \Phi_{2k,l}(j)} \gamma\left(\frac{r_{k,\rho}^2}{\sigma_z^2 + \sigma_h^2 q}, k\right) \end{aligned} \tag{16}$$

where $\Phi_{2k,l}(q)$ is the coefficient of x^q in the polynomial $(\phi_1(x))^l (\phi_2(x))^{2k-l}$, $\phi_1(x) = 1 + x + x^4 + x^9$, $\phi_2(x) = 1 + 2x + x^4$ and $\gamma(x, k) = \int_0^x \left(\lambda^{k-1}/\Gamma(k)\right) \mathrm{e}^{-\lambda}\, \mathrm{d}\lambda$.

Proof: See Appendix 2. □

3.4 Construction of upper bound on expected complexity

We are ready to construct the final form of the upper bound on the expected IRA complexity by assembling our analytical results. Let us consider the summation term $\sum_{\boldsymbol{x}^{(k)}} \Pr(P_k(\boldsymbol{x}^{(k)}) \le r_{k,\rho}^2)$ in (11). First, by specifying the transmitted vector $\bar{\boldsymbol{x}}$ together with (2), $\boldsymbol{w}$ can be rewritten as $\boldsymbol{w} = \boldsymbol{Q}^* \boldsymbol{y} - \boldsymbol{R}\boldsymbol{x} = \boldsymbol{R}\boldsymbol{d} + \boldsymbol{v}$, where $\boldsymbol{d} = \bar{\boldsymbol{x}} - \boldsymbol{x}$ and $\boldsymbol{v} = \boldsymbol{Q}^* \boldsymbol{z}$; thus, it follows from the definition of path metric that $P_k(\boldsymbol{d}^{(k)}) = \|\boldsymbol{R}_{(k)} \boldsymbol{d}^{(k)} + \boldsymbol{v}^{(k)}\|^2$, where $\boldsymbol{R}_{(k)}$ is a $k \times k$ lower right submatrix of $\boldsymbol{R}$. Subsequently, we consider the conditioning of the transmitted subvector $\bar{\boldsymbol{x}}^{(k)}$, whereby $\Pr(P_k(\boldsymbol{x}^{(k)}) \le r_{k,\rho}^2 | \bar{\boldsymbol{x}}^{(k)}) = \Pr(P_k(\boldsymbol{d}^{(k)}) \le r_{k,\rho}^2)$. As a result, $\sum_{\boldsymbol{x}^{(k)}} \Pr(P_k(\boldsymbol{x}^{(k)}) \le r_{k,\rho}^2)$ is rewritten as

$$\begin{aligned} \sum_{\boldsymbol{x}^{(k)}} \Pr\left(P_k\left(\boldsymbol{x}^{(k)}\right) \le r_{k,\rho}^2\right) &= \sum_{\boldsymbol{x}^{(k)}} \frac{1}{L^{2k}} \Pr\left(P_k\left(\boldsymbol{x}^{(k)}\right) \le r_{k,\rho}^2 | \bar{\boldsymbol{x}}^{(k)}\right) \\ &= \sum_{\boldsymbol{d}^{(k)}} \frac{1}{L^{2k}} \Pr\left(P_k\left(\boldsymbol{d}^{(k)}\right) \le r_{k,\rho}^2\right) \end{aligned}$$

where $\bar{\boldsymbol{x}}^{(k)}$ is assumed to be equally likely transmitted with a probability $1/L^{2k}$. We denote the average number of pairs $\left(\bar{\boldsymbol{x}}^{(k)}, \boldsymbol{x}^{(k)}\right)$ such that $\|\bar{\boldsymbol{x}}^{(k)} - \boldsymbol{x}^{(k)}\|^2 = q$ as $n_k(q)$. Then, without any loss of generality, we obtain

$$\sum_{\boldsymbol{x}^{(k)}} \Pr\left(P_k\left(\boldsymbol{x}^{(k)}\right) \le r_{k,\rho}^2\right) = \sum_q n_k(q) \gamma\left(\frac{r_{k,\rho}^2}{\sigma_z^2 + \sigma_h^2 q}, k\right) \tag{17}$$

In (17), $n_k(q)$ is given by $\binom{2k}{q}$ for the 4-QAM constellation, as mentioned in the proof of Theorem 1. In addition, we obtain

$$n_k(q) = \sum_{l=0}^{2k} \binom{2k}{l} \frac{1}{4^k} \Phi_{2k,l}(q)$$

for the 16-QAM constellation by using (27) and the fact that the number of $\left(\bar{\boldsymbol{x}}^{(k)}, \boldsymbol{x}^{(k)}\right)$ satisfying $\|\bar{\boldsymbol{x}}^{(k)} - \boldsymbol{x}^{(k)}\|^2 = q$, given the occurrence of event $\boldsymbol{A}_{2k,l}$, is $\Phi_{2k,\,l}(q)$.

Finally, by incorporating (12) and (17) into (11), the expected complexity C in the 4-QAM constellation is found to be upper bounded by

$$\begin{aligned} C \le {} & \sum_{\rho=1}^{N_s} \left(\mathrm{P}_{\mathrm{UB},\rho-1} - \mathrm{P}_{\mathrm{LB},\rho}\right) \\ & \times \sum_{k=1}^{M} \sum_{q=0}^{2k} \binom{2k}{q} \gamma\left(\frac{r_{k,\rho}^2}{\sigma_z^2 + \sigma_h^2 q}, k\right) f(k) \end{aligned} \tag{18}$$

Subsequently, similar to the 4-QAM constellation case, we obtain the following upper bound for the 16-QAM

doi: 10.1049/iet-com.2012.0232

constellation

$$C \le \sum_{\rho=1}^{N_s}\left(\mathrm{P}_{\mathrm{UB},\rho-1} - \mathrm{P}_{\mathrm{LB},\rho}\right)\sum_{k=1}^{M}\sum_{q=0}^{18k}\sum_{l=0}^{2k}\frac{\binom{2k}{l}}{4^k} \Phi_{2k,l}(q)\gamma\left(\frac{r_{k,\rho}^2}{\sigma_z^2+\sigma_h^2 q}, k\right) f(k) \quad (19)$$

We remind that in (18) and (19), $w(\rho) = P_{\mathrm{UB},\rho-1} - P_{\mathrm{LB},\rho}$ can be computed using the results given by Theorem 1.

4 Numerical results

In this section, we present numerical results and identify the difference between our IRA complexity analysis and that presented in [10]. Further, the analytical results are compared with the results obtained by Monte Carlo simulations. Here, the expected complexity C is presented through the complexity exponent $\log(C)/\log(L^2)$ for the L^2-QAM constellations. For presenting the analysis and simulation results, the probability ε_ρ is determined as 0.1, 0.01, 0.001, 0.0, and thus, $N_s = 4$. This exponentially decreasing schedule of ε_ρ was also used to present numerical results in [10–12]. In all the simulations, we generated at least 50 000 channel realisations for each SNR point or number of transmit antennas.

Fig. 3 illustrates the new upper bound on the expected complexity [i.e. (18)] and the simulated average complexity, obtained by varying the SNR in a 10×10 MIMO system with a 4-QAM constellation. As seen in Fig. 3, the analysis and simulation results show a decreasing trend for high SNRs. Note that our analysis result consistently presents a valid upper bound with respect to the simulation result. This consistency is maintained over all SNRs.

In Fig. 4, we compare the new upper complexity bound [i.e. (19)] with the result of the complexity analysis given for one fixed ρ [10] in an 8×8 MIMO system with a 16-QAM constellation. The analysis result in [10] shows different values according to the selected radius schedule (or the specific value of ρ), as seen in Fig. 4. The analytical results for $\rho = 3$, 4 maintain an upper bound with respect to the simulated complexity over all SNRs. For the analysis results with $\rho = 3$, 4, even though the result for $\rho = 3$ appears close to the simulation result shown in Fig. 4, it is noteworthy that this specific value of ρ, which provides a corresponding upper bound, can be known after performing extensive simulation experiments and subsequent comparisons between the analysis and simulation results. On the other hand, the new upper bound is not ambiguous

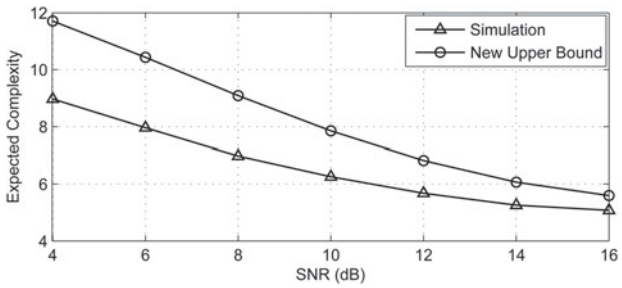

Fig. 3 *Expected complexity against SNR in a 10×10 MIMO system with 4-QAM*

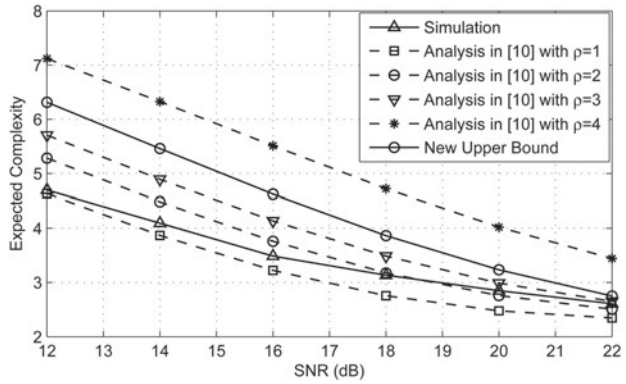

Fig. 4 *Expected complexity against SNR in an 8×8 MIMO system with 16-QAM*

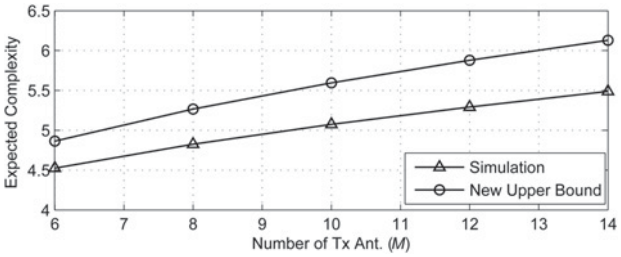

Fig. 5 *Expected complexity against M in a MIMO system with 4-QAM at SNR = 16 dB*

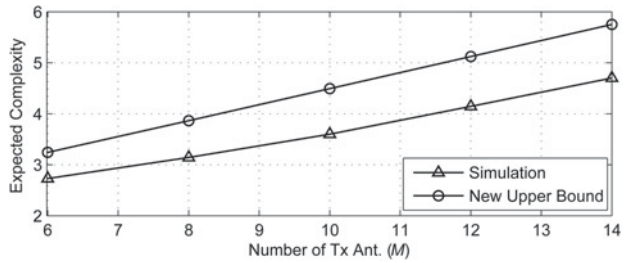

Fig. 6 *Expected complexity against M in a MIMO system with 16-QAM at SNR = 18 dB*

with respect to the radius schedule because we considered the randomness of the radius schedule during our analysis. Therefore our upper bound is more practical for evaluating an actual system that includes radius schedule variation.

Figs. 5 and 6 plot the new upper bounds of (18) and (19) and the simulated complexity at a fixed SNR by increasing the number of transmit antennas, M, for 4-QAM and 16-QAM constellations, respectively. We again observe that our upper bounds provide a good prediction over different M. In Figs. 5 and 6, both the analytical and simulated result curves show a similar tendency that the complexity is exponentially increased with M at a fixed SNR. From the numerical results and discussions presented above, we believe that our analysis results are useful as analytical tools for understanding complexity behaviour in a more realistic manner.

5 Conclusion

In this paper, we presented a new analysis for evaluating the expected IRA complexity that considers the usage of multiple

radius schedules. In contrast to the previous analysis, where the radius schedule was hypothetically fixed for analytic convenience, our analytical method reflects the effect of the random variation in the radius schedule, which is one of the IRAs operational characteristics. The derived results on the expected complexity were validated for various system configurations and agreed well with the simulated results. Hence, our analysis can be used to provide reliable complexity estimation without any ambiguity related to the radius schedule and offer a better understanding of algorithmic complexity.

6 Acknowledgments

This work was supported by the Basic Research Project through a grant provided by GIST, and by the World Class University (WCU) program at GIST through a grant provided by the Ministry of Education, Science and Technology (MEST) of Korea (Project No. R31-10026), and partially by a research grant (UD1000211D) of the Agency for Defense Development (ADD), Korea.

7 References

1 Hassibi, B., Vikalo, H.: 'On the sphere decoding algorithm. Part I: The expected complexity', *IEEE Trans. Signal Process.*, 2005, **53**, (8), pp. 2806–2818
2 Chang, X.-W., Han, Q.: 'Solving box-constrained integer least squares problems', *IEEE Trans. Wirel. Commun.*, 2008, **7**, (1), pp. 277–287
3 Damen, M.O., Gamel, H.E., Caire, G.: 'On maximum-likelihood detection and the search for the closest lattice point', *IEEE Trans. Inf. Theory*, 2003, **49**, (10), pp. 2389–2402
4 Windpassinger, C., Lampe, L., Fischer, R., Hehn, T.: 'A performance study of MIMO detectors', *IEEE Trans. Wirel. Commun.*, 2006, **5**, (8), pp. 2004–2008
5 Barbero, L.G., Thompson, J.S.: 'Performance of the complex sphere decoder in spatially correlated MIMO channels', *IET Commun.*, 2007, **1**, (1), pp. 122–130
6 Brunel, L.: 'Multiuser detection techniques using maximum likelihood sphere decoding in multicarrier CDMA systems', *IEEE Trans. Wirel. Commun.*, 2004, **3**, (3), pp. 949–957
7 Mow, W.: 'Maximum likelihood sequence estimation from the lattice viewpoint', *IEEE Trans. Inf. Theory*, 1994, **40**, (5), pp. 1591–1600
8 Ajtai, M.: 'The shortest vector problem in L_2 is NP-hard for randomized reductions'. Proc. 30th Annual ACM Symp. on Theory of Computing, Dallas, TX, USA, May 1998, pp. 10–19
9 Agrell, E., Eriksson, T., Vardy, A., Zeger, K.: 'Closest point search in lattices', *IEEE Trans. Inf. Theory*, 2002, **48**, (8), pp. 2201–2214
10 Gowaikar, R., Hassibi, B.: 'Statistical pruning for near-maximum likelihood decoding', *IEEE Trans. Signal Process.*, 2007, **55**, (6), pp. 2661–2675
11 Ghaderipoor, A., Tellambura, C.: 'A statistical pruning strategy for Schnorr-Euchner sphere decoding', *IEEE Commun. Lett.*, 2008, **12**, (2), pp. 121–123
12 Liang, Y., Ma, S., Ng, T.-S.: 'Low complexity near-maximum likelihood decoding for MIMO systems'. Proc. IEEE PIMRC, Tokyo, Japan, September 2009, pp. 2429–2433
13 Seethaler, D., Bölcskei, H.: 'Performance and complexity analysis of infinity-norm sphere-decoding', *IEEE Trans. Inf. Theory*, 2010, **56**, (3), pp. 1085–1105

8 Appendix

8.1 Appendix 1 Determination of the weight $w(\rho)$:

A search success event in the radius schedule having index ρ implies that IRA fails to find a solution for the previous schedule indexes from 1 to $\rho-1$. However, it eventually succeeds in searching for a solution in the radius schedule with index ρ. Recall that $\mathcal{D}_{k,\rho-1} \subseteq \mathcal{D}_{k,\rho}$ for all k; thus, $\Pr(\mathcal{D}_{M,\rho-1} = \emptyset | \mathcal{D}_{M,\rho} = \emptyset) = 1$. From this fact, the search success probability in the radius schedule with index ρ is given by

$$\Pr\left(\mathcal{D}_{M,1} = \emptyset, \mathcal{D}_{M,2} = \emptyset, \ \ldots, \mathcal{D}_{M,\rho-1} = \emptyset, \mathcal{D}_{M,\rho} \neq \emptyset\right) = \Pr\left(\mathcal{D}_{M,\rho-1} = \emptyset, \mathcal{D}_{M,\rho} \neq \emptyset\right) \tag{20}$$

where $\rho = 1, 2, \ldots, N_s$, $\Pr(\mathcal{D}_{M,0} = \emptyset, \mathcal{D}_{M,1} \neq \emptyset) = \Pr(\mathcal{D}_{M,1} \neq \emptyset)$ by definition. From the total probability theorem together with $\Pr(\mathcal{D}_{M,\rho} \neq \emptyset | \mathcal{D}_{M,\rho-1} \neq \emptyset) = 1$, we know that

$$\Pr(\mathcal{D}_{M,\rho} \neq \emptyset) = \Pr(\mathcal{D}_{M,\rho} \neq \emptyset | \mathcal{D}_{M,\rho-1} = \emptyset) \Pr(\mathcal{D}_{M,\rho-1} = \emptyset) + \Pr(\mathcal{D}_{M,\rho-1} \neq \emptyset)$$

which leads to

$$\Pr\left(\mathcal{D}_{M,\rho} \neq \emptyset | \mathcal{D}_{M,\rho-1} = \emptyset\right) = \frac{\Pr\left(\mathcal{D}_{M,\rho} \neq \emptyset\right) - \Pr\left(\mathcal{D}_{M,\rho-1} \neq \emptyset\right)}{\Pr\left(\mathcal{D}_{M,\rho-1} = \emptyset\right)} \tag{21}$$

Subsequently, multiplying (21) by $\Pr(\mathcal{D}_{M,\rho-1} = \emptyset)$ together with $\Pr(\mathcal{D}_{M,\rho} = \emptyset) = 1 - \Pr(\mathcal{D}_{M,\rho} \neq \emptyset)$ yields

$$\Pr\left(\mathcal{D}_{M,\rho-1} = \emptyset, \mathcal{D}_{M,\rho} \neq \emptyset\right) = \Pr\left(\mathcal{D}_{M,\rho-1} = \emptyset\right) - \Pr\left(\mathcal{D}_{M,\rho} = \emptyset\right) \tag{22}$$

where $\Pr(\mathcal{D}_{M,0} = \emptyset) = 1$ by definition.

Let us evaluate the upper bound on $\Pr(\mathcal{D}_{M,\rho-1} = \emptyset, \mathcal{D}_{M,\rho} \neq \emptyset t)$ in (22), which is obtained by $P_{\mathrm{UB},\rho-1} - P_{\mathrm{LB},\rho}$, where $P_{\mathrm{UB},\rho-1}$ and $P_{\mathrm{LB},\rho}$ denote an upper bound on $\Pr(\mathcal{D}_{M,\rho-1} = \emptyset)$ and a lower bound on $\Pr(\mathcal{D}_{M,\rho} = \emptyset)$, respectively. First, $\Pr(\mathcal{D}_{M,\rho} = \emptyset)$ is expanded as

$$\Pr\left(\mathcal{D}_{M,\rho} = \emptyset\right) = \Pr(\mathcal{D}_{1,\rho} = \emptyset) + \sum_{k=2}^{M} \Pr\left(\mathcal{D}_{k,\rho} = \emptyset | \mathcal{D}_{k-1,\rho} \neq \emptyset\right) \Pr\left(\mathcal{D}_{k-1,\rho} \neq \emptyset\right) \tag{23}$$

where from the definition of the search space $\mathcal{D}_{k,\rho}$, $\Pr(\mathcal{D}_{1,\rho} = \emptyset)$, $\Pr(\mathcal{D}_{k,\rho} = \emptyset | \mathcal{D}_{k-1,\rho} \neq \emptyset)$, and $\Pr(\mathcal{D}_{k-1,\rho} \neq \emptyset)$ are equivalent to $\Pr(P_1(\boldsymbol{x}^{(1)}) > r_{1,\rho}^2)$, $\Pr(P_k(\boldsymbol{x}^{(k)}) > r_{k,\rho}^2)$, and $\Pr(\bigcap_{j=1}^{k-1}\{P_j(\boldsymbol{x}^{(j)}) \leq r_{j,\rho}^2\})$, respectively, and $\boldsymbol{x}^{(k)} \in \mathcal{S}^k$ is the uniformly distributed random variable of realisation $\boldsymbol{x}^{(k)}$. Then, the lower bound on $\Pr(\mathcal{D}_{M,\rho} = \emptyset)$ in (23) is given by (13). From (23) together with the inequality $\Pr(\bigcap_{j=1}^{k-1}\{P_j(\boldsymbol{x}^{(j)}) \leq r_{j,\rho-1}^2\}) \leq \Pr(P_{k-1}(\boldsymbol{x}^{(k-1)}) \leq r_{k-1,\rho-1}^2)$, the upper bound on $\Pr(\mathcal{D}_{M,\rho-1} = \emptyset)$ results in (14). Subsequently, subtracting (13) from (14) yields the upper bound on $\Pr(\mathcal{D}_{M,\rho-1} = \emptyset, \mathcal{D}_{M,\rho} \neq \emptyset)$, which is labelled as the computational weight $w(\rho)$, as in (12).

8.2 Appendix 2: Proof of Theorem 1:

The random variable $2P_k(\boldsymbol{x}^{(k)})/(\sigma_z^2 + \sigma_h^2\|\bar{\boldsymbol{x}}^{(k)} - \boldsymbol{x}^{(k)}\|^2)$ follows the χ^2

doi: 10.1049/iet-com.2012.0232

distribution with $2k$ degrees of freedom, that is $2P_k(\boldsymbol{x}^{(k)})/(\sigma_z^2+\sigma_h^2\|\bar{\boldsymbol{x}}^{(k)}-\boldsymbol{x}^{(k)}\|^2)\sim\chi^2_{2k}$, where $\bar{\boldsymbol{x}}^{(k)}=[\bar{x}_{M-k+1},\ \bar{x}_{M-k+2},\ \ldots,\bar{x}_M]^{\mathrm{T}}$ [1, 10]. Hence, the following equation is obtained

$$\Pr\left(P_k\left(\boldsymbol{x}^{(k)}\right)\le r_{k,\rho}^2\right)=\gamma\left(\frac{r_{k,\rho}^2}{\sigma_z^2+\sigma_h^2\|\bar{\boldsymbol{x}}^{(k)}-\boldsymbol{x}^{(k)}\|^2},k\right) \quad (24)$$

Then, using the total probability theorem, (24) is rewritten as

$$\Pr\left(P_k\left(\boldsymbol{x}^{(k)}\right)\le r_{k,\rho}^2\right)=\sum_q \Pr\left(\|\bar{\boldsymbol{x}}^{(k)}-\boldsymbol{x}^{(k)}\|^2=q\right)\gamma\left(\frac{r_{k,\rho}^2}{\sigma_z^2+\sigma_h^2 q},k\right) \quad (25)$$

where $\sum_q$ denotes the sum over all possible q, and $\Pr\left(\|\bar{\boldsymbol{x}}^{(k)}-\boldsymbol{x}^{(k)}\|^2=q\right)$ is the probability of a pair $\left(\bar{\boldsymbol{x}}^{(k)},\boldsymbol{x}^{(k)}\right)$ satisfying $\|\bar{\boldsymbol{x}}^{(k)}-\boldsymbol{x}^{(k)}\|^2=q$, which is derived below in detail for each constellation.

• *4-QAM constellation*: Consider 4-QAM constellation points $x_k=x_{k,1}+jx_{k,2}$ and $\bar{x}_k=\bar{x}_{k,1}+j\bar{x}_{k,2}$, where $x_{k,1},x_{k,2},\bar{x}_{k,1},\bar{x}_{k,2}\in\{-1/2,1/2\}$. The real and imaginary parts of each entry of the term $\bar{\boldsymbol{x}}^{(k)}-\boldsymbol{x}^{(k)}$ in (25) have only two possible values $\{0,1\}$ with equal probability, respectively. Thus, the number of pairs $\left(\bar{\boldsymbol{x}}^{(k)},\boldsymbol{x}^{(k)}\right)$ complying with $\|\bar{\boldsymbol{x}}^{(k)}-\boldsymbol{x}^{(k)}\|^2=q$ is $\binom{2k}{q}$. Then, since the total number of $\left(\bar{\boldsymbol{x}}^{(k)},\boldsymbol{x}^{(k)}\right)$ for all possible values of $\|\bar{\boldsymbol{x}}^{(k)}-\boldsymbol{x}^{(k)}\|^2$ is given by $\sum_{j=0}^{2k}\binom{2k}{j}=4^k$, we obtain

$$\Pr\left(\|\bar{\boldsymbol{x}}^{(k)}-\boldsymbol{x}^{(k)}\|^2=q\right)=\frac{\binom{2k}{q}}{4^k} \quad (26)$$

By substituting (26) into (25), $\Pr(P_k(\boldsymbol{x}^{(k)})\le r_{k,\rho}^2)$ for the 4-QAM constellation is derived as (15).

• *16-QAM constellation*: Recall 16-QAM constellation points $x_k=x_{k,1}+jx_{k,2}$ and $\bar{x}_k=\bar{x}_{k,1}+j\bar{x}_{k,2}$, where $x_{k,1},x_{k,2},\bar{x}_{k,1},\bar{x}_{k,2}\in\{-3/2,-1/2,1/2,3/2\}$. For each $\bar{x}_{k,1}$ and $\bar{x}_{k,2}$ (or $x_{k,1}$ and $x_{k,2}$), the pairs $-3/2$, $3/2$ and $-1/2$, $1/2$ are referred to as the corner and centre points, respectively. We subsequently define an event $A_{2k,l}$ as 'select a corner point l times from among the $2k$ entries of the real and imaginary parts of $\bar{\boldsymbol{x}}^{(k)}$'. The probability of event $A_{2k,l}$ is given by

$$\Pr\left(A_{2k,l}\right)=\frac{\binom{2k}{l}}{4^k} \quad (27)$$

Let us evaluate the number of pairs $\left(\bar{\boldsymbol{x}}^{(k)},\boldsymbol{x}^{(k)}\right)$ satisfying $\|\bar{\boldsymbol{x}}^{(k)}-\boldsymbol{x}^{(k)}\|^2=q$, given the occurrence of the event $A_{2k,l}$. To do this, we take advantage of the generating polynomial expansion, which was named as the modified Euler's generating function technique in [1]. When $\bar{x}_{k,1}$ (or $\bar{x}_{k,2}$) is selected as a corner point, it follows that $|\bar{x}_{k,1}-x_{k,1}|^2$ (or $|\bar{x}_{k,2}-x_{k,2}|^2)\in\{0,1,4,9\}$. Conversely, if $\bar{x}_{k,1}$ (or $\bar{x}_{k,2}$) is chosen as a centre point, then $|\bar{x}_{k,1}-x_{k,1}|^2$ $(\text{or}|\bar{x}_{k,2}-x_{k,2}|^2)\in\{0,1,1,4\}$. Thus, the generating polynomials for the corner and centre points are given by $\phi_1(x)=1+x+x^4+x^9$ and $\phi_2(x)=1+2x+x^4$, respectively, where the exponents in these functions indicate information on the possible values of $|\bar{x}_{k,1}-x_{k,1}|^2$ (or $|\bar{x}_{k,2}-x_{k,2}|^2$), and the coefficients in these functions represent the number of pairs $\left(\bar{x}_{k,1},x_{k,1}\right)$ (or $\left(\bar{x}_{k,2},x_{k,2}\right)$) that have specific values of $|\bar{x}_{k,1}-x_{k,1}|^2$ (or $|\bar{x}_{k,2}-x_{k,2}|^2$). Let us consider the generating polynomial expansion of $(\phi_1(x))^l(\phi_2(x))^{2k-l}$ for the general case of $\left(\bar{\boldsymbol{x}}^{(k)},\boldsymbol{x}^{(k)}\right)$, and denote as $\Phi_{2k,l}(q)$, the coefficient of x^q in $(\phi_1(x))^l(\phi_2(x))^{2k-l}$. Then, $\Phi_{2k,l}(q)$ corresponds to the number of pairs $\left(\bar{\boldsymbol{x}}^{(k)},\boldsymbol{x}^{(k)}\right)$ satisfying $\|\bar{\boldsymbol{x}}^{(k)}-\boldsymbol{x}^{(k)}\|^2=q$, given the occurrence of event $A_{2k,l}$. Further, assuming the occurrence of event $A_{2k,l}$, the total number of combinations for all possible values of $\|\bar{\boldsymbol{x}}^{(k)}-\boldsymbol{x}^{(k)}\|^2$ is $\Sigma_j\Phi_{2k,l}(j)$, where Σ_j denotes the sum over all possible j. Thus, it follows from the above discussion that

$$\Pr\left(\|\bar{\boldsymbol{x}}^{(k)}-\boldsymbol{x}^{(k)}\|^2=q|A_{2k,l}\right)=\frac{\Phi_{2k,l}(q)}{\sum_j\Phi_{2k,l}(j)} \quad (28)$$

Using (27), (28), and the total probability theorem, we have

$$\Pr\left(\|\bar{\boldsymbol{x}}^{(k)}-\boldsymbol{x}^{(k)}\|^2=q\right)=\sum_{l=0}^{2k}\frac{\binom{2k}{l}}{4^k}\frac{\Phi_{2k,l}(q)}{\sum_j\Phi_{2k,l}(j)} \quad (29)$$

Finally, by incorporating (29) into (25), $\Pr(P_k(\boldsymbol{x}^{(k)})\le r_{k,\rho}^2)$ for the 16-QAM constellation is given by (16).